9th International Particle Accelerator Conference IPAC2018, Vancouver, BC, Canada JACoW Publishing
ISBN: 978-3-95450-184-7 doi:10.18429/JACoW-IPAC2018-MOYGB2

The LCLS-II: A HIGH POWER UPGRADE TO THE LCLS*

John N. Galayda†, SLAC National Accelerator Laboratory, Menlo Park, CA 94025, USA
representing the LCLS-II collaboration (ANL, Lemont IL 60439; FNAL, Batavia IL 60510; Jefferson Lab, Newport News VA 23606; LBNL, Berkeley, CA 94720; and Cornell University, Ithaca NY 14850 USA)

Abstract

The LCLS-II is an upgrade of the Linac Coherent Light Source (LCLS) X-ray FEL based on a 4 GeV superconducting RF linac. The LCLS-II is designed to produce hundreds of watts of X-rays from 200 eV up to 5 keV. The linac uses 1.3 GHz 9-cell cavities processed using the N_2-doping technique, and will be the first large-scale CW SCRF linac with a Q of roughly 3 x 10^{10} at a gradient of 16 MV/m. The injector, which will be commissioned in spring 2018, is based on the normal-conducting CW RF APEX gun developed at LBNL. The LCLS-II will have two undulators: The soft X-ray undulator is a 39 mm period hybrid PM with an adjustable vertical gap to cover the range from 200 eV to 1.5 keV, and the hard X-ray undulator is a novel adjustable horizontal gap hybrid PM undulator with 26 mm period to generate vertically polarized X-rays from 1 to 5 keV. The talk will review the performance goals as well as some notable aspects of hardware fabrication.

INITIATION, COST & SCHEDULE

The Linac Coherent Light Source (LCLS) produced first X-rays in 2009, and quickly proved to be an effective research tool [1]. In July 2013, the Department of Energy Office of Science (DOE-SC) received a report [2] from its Basic Energy Sciences Advisory Committee recommending the construction of an X-ray FEL user facility with pulse repetition rate up to 1 MHz, beyond the capabilities of the 120 Hz SLAC linac. A collaboration of physicists and engineers from US accelerator laboratories (ANL, Cornell University, FNAL, JLAB, LBNL and SLAC) met for the first time in October 2013 to plan the construction of a free-electron laser employing a superconducting linac at SLAC. DOE-SC approved the conceptual design [3] of LCLS-II in August 2014. Construction began in March 2016, with the goal of completing the project no later than June 2022. The project budget is $1,045M, inclusive of materials, labor, civil construction and commissioning.

PROJECT DESCRIPTION

X-Ray Spectral Range

The LCLS-II project must create two simultaneously operable X-ray sources, each producing evenly spaced pulses at rates up to ~1 MHz. One source will produce 200-1,300 eV X-rays and the other will span the spectrum from 1 keV to 5 keV.

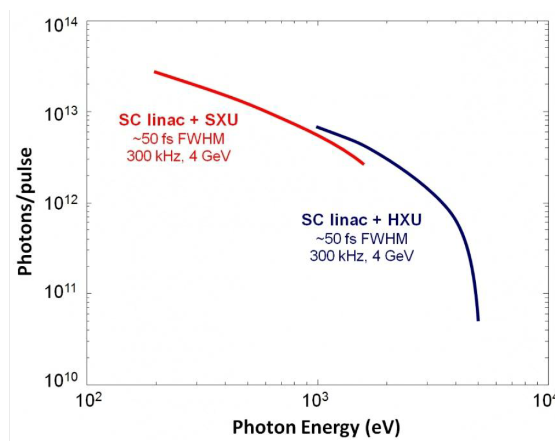

Figure 1: Tuning range and estimated maximum photons/pulse from the two new undulators, using the superconducting LCLS-II linac. The linac can provide pulses at rates up to ~1 MHz. The number of photons/pulse at a given photon energy will vary in rough proportion to the desired pulse duration, which will range from 1fs to 100fs.

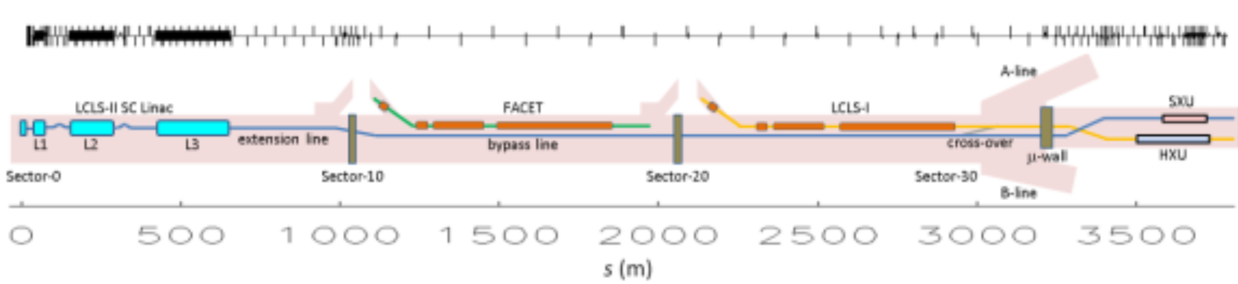

Figure 2: The LCLS-II linac occupies the first 700 m of the SLAC linac tunnel. An existing transport line carries electrons past the remaining two 1-km segments of the original copper linac. A plasma wakefield acceleration experiment (FACET-II) will occupy the middle segment of the linac. The third segment is the LCLS linac, which will provide an alternative source of higher-energy electrons to the LCLS facility.

* Work supported by the U.S. Department of Energy under contract DE-AC02-768F00515.
† galayda@slac.stanford.edu

ISBN: 978-3-95450-184-7 doi:10.18429/JACoW-IPAC2018-MOYGB2

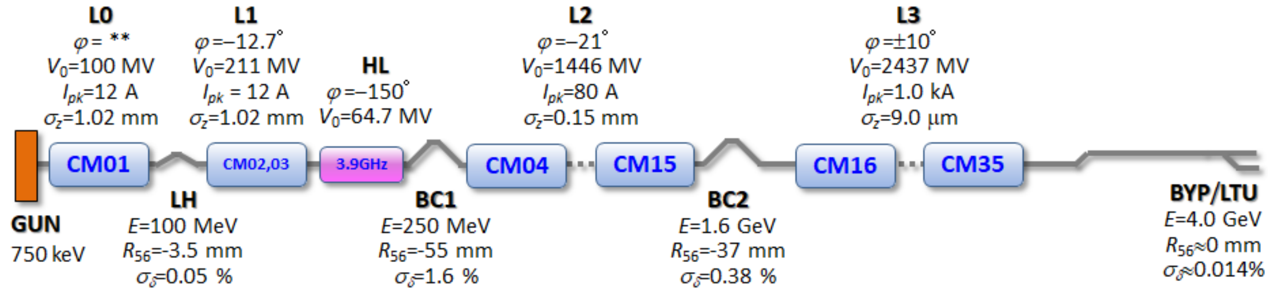

Figure 3: Schematic of the LCLS-II linac showing placement of 1.3 GHz cryomodules (CM01-CM35) and chicanes for the laser heater (LH) and bunch compressors (BC1, BC2). L0 is a single cryomodule 2 m downstream of the gun. L1, L2 and L3 are cryogenically integrated segments of the linac with two, 12 and 20 cryomodules respectively. HL represents two cryomodules with 3.9 GHz cavities that prepare the electron longitudinal phase space for bunch compression.

Facility Overview

LCLS-II will make extensive use of existing infrastructure at SLAC. The project has removed equipment from the first kilometer of the 3 km SLAC linac tunnel and klystron gallery and is now installing the new accelerator (see Fig. 1). A laser room and photocathode injector source have been installed in place of the original SLAC injector. A 4 GeV superconducting linear accelerator [4] will fill approximately 700 m of this 1-km segment of the tunnel. All S-band klystron systems have been replaced with solid-state RF sources and computer controls in the klystron gallery above the tunnel. Electrons from this linac will be transported past the remaining 2-km S-band linac facilities through a transport line originally built for filling the PEP and PEP-II rings. A fanout kicker will direct electron bunches to two transport lines at rates up to 1 MHz each. These lines will pass through the Beam Transport Hall (originally built for the LCLS facility) to the LCLS Undulator Hall. The original LCLS undulator will be replaced with two new undulators. With electrons from the SC linac, these two undulator sources [5] (SXU and HXU in Fig. 1) will effectively double the experimental capacity of the LCLS facility.

The copper S-band linac that has provided electrons to LCLS will remain available as an alternate source of electrons for the new hard X-ray undulator, providing X-ray pulses of up to 25 keV at 120 Hz.

Electron beam containment systems and beam dumps will be upgraded to safely transport and dump electron beam powers up to 120 kW through each undulator. LCLS-II and the LCLS facility are closely coordinating plans and activities. LCLS optics are being continuously upgraded to meet the needs of current operations and to facilitate the transition to operation with the higher average beam powers of LCLS-II.

The cryogenic refrigeration plant for the linac is being installed in a new building on the north side of the linac, about 400 m downstream of the electron injector.

Electron Injector

The electron source for LCLS-II is a 186 MHz CW RF gun developed and built by LBNL [6]. It is closely patterned after the APEX gun, which has been operating at LBNL in support of ultrafast electron diffraction research. The electron source is now installed in the linac tunnel (Fig. 3) and will produce first electrons in August 2018 [7].

Figure 4: The LCLS-II electron gun (in the foreground) installed in the linac tunnel. Visible are the optics hutch for the cathode (right side) and the end cap (painted blue) for the first cryomodule, which is not yet installed.

Linac and Cryomodules

The LCLS-II accelerating cryomodules are very similar to the cryomodules developed for the International Linear Collider and the European XFEL, with modifications needed for CW operation [8] (see Fig. 6). Thirty-five 1.3 GHz cryomodules (nominal gradient 16 MV/m) and two 3.9 GHz cryomodules (72 MV/m on-crest) will accelerate electrons to 4 GeV. To date, FNAL has constructed nine cryomodules and tested eight [9]; JLAB has constructed and tested seven cryomodules.

The geometry of the 1.3 GHz cavities is identical to European XFEL. The cavity helium vessel includes modifications to permit tuning with a FNAL-designed lever tuner [10]. The fundamental and higher-mode couplers

ISBN: 978-3-95450-184-7 doi:10.18429/JACoW-IPAC2018-MOYGB2

are nearly identical to European XFEL. The insulating vacuum vessel resembles European XFEL units with the addition of eight access ports that may be used to replace tuner motors if necessary. The quadrupole magnet is a Fermilab/KEK design that can be split so that it may be installed outside the cleanroom.

Modifications for CW operation include larger-diameter 2-phase pipe, which cannot be connected from cryomodule to cryomodule because the SLAC linac tunnel was constructed on a 4 milliradian downhill slope.

The LCLS-II cryomodule has no 5 K shield; since the dominant heat load comes from the cavities (80 W at 2 K), interception of this heat load on a 5 K surface has no benefit for LCLS-II.

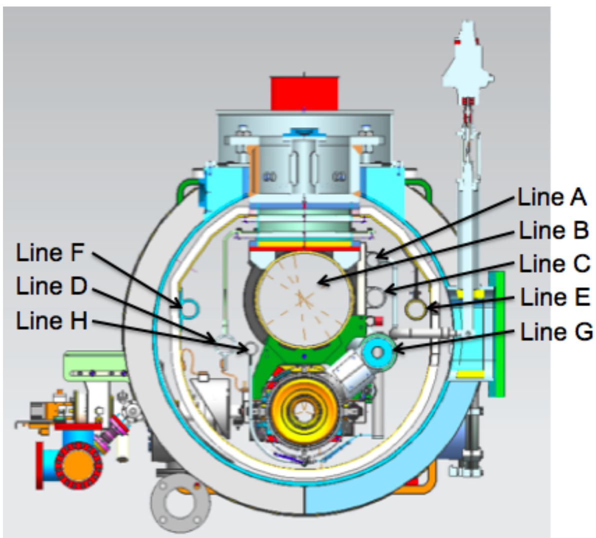

Figure 5: Cross-section of the LCLS-II cryomodule. Line A: 2.4 K subcooled supply; Line B: Helium gas return pipe (HGRP); Line C: Low-temperature intercept supply; Line D: Low-temperature intercept return; Line E: High-temperature shield supply; Line F: High -temperature shield return: Line G: 2-phase pipe; Line H: Warm-up/cool-down line

Nitrogen Doping and Cavity Quality Factor

The most influential performance requirements for LCLS-II are consequences of CW operation. To ensure that LCLS-II will run at 4 GeV in CW mode, the project is building two cryoplants, designed and acquired by JLAB [11]. Together, the LCLS-II plants will provide ~8 kW cooling capacity at 2 K.

While 2 x 4 kW cooling at 2 K is sufficient to guarantee operation at 4 GeV with high confidence, the project also invested in implementation of a recent discovery that would make it possible to operate the linac at 4 GeV while cooled by a single cryoplant, reducing facility operations costs by at least \$3M/year. Operation of LCLS-II with one cryoplant would be feasible if the ensemble average of cavity Q's in the linac could be held at or above 2.7 x 10^{10}. A recent discovery, nitrogen doping, promised to make this possible. The doping treatment could be straightforwardly applied to the cavities during final baking at the manufacturers. Q measurements of LCLS-II production cavities at JLAB and FNAL demonstrate average Q's for > 100 nitrogen-doped 1.3 GHz cavities of just over 3 x 10^{10} at 16 MV/m, the nominal LCLS-II operating gradient. LCLS-II committed to exploit this discovery at the start of facility design. To ensure that the accelerator could operate CW with a single cryoplant, the project set a target of $<Q>= 2.7 \times 10^{10}$ for the ensemble average of cavities in the linac.

The LCLS-II collaboration embarked on an intense R&D period, the goal of which was to demonstrate and industrialize the nitrogen doping process for application to LCLS-II cavities [12]. A series of trials using single-cell cavities led to a candidate doping recipe for LCLS-II. The recipe was tested on sixteen 9-cell cavities, which had been built several years earlier as part of the International Linear Collider (ILC) research collaboration. Q measurements were performed on these cavities in vertical orientation with excellent results. The first two LCLS-II cryomodules, built at FNAL and JLAB, respectively, exhibited average Q of 3 x 10^{10} and 2.9 x 10^{10} along with maximum gradient above 19 MV/m – very satisfactory indeed.

Flux Trapping at Superconducting Transition

Nitrogen doping enables the achievement of high Q, providing that ambient magnetic fields around the cavity are kept near zero during the transition to superconductivity. Trapped flux reduces both the Q value and the quench gradient of the cavity; the benefits of doping can be lost if magnetic flux becomes trapped in localized flux tubes in the cavity. A 1-mG field permeating the cavity, if trapped at transition, contributes about 1.4 nΩ to the effective cavity shunt resistance. The project set a goal of reducing ambient field on the cavities in the cryomodule below 5 mG. Even with this low ambient field, the target Q value could be reached only if the Meissner effect would expel most of the remaining ambient flux from the niobium cells and cavities at transition to superconductivity.

Success in expulsion of flux depends on details of the time evolution of spatial temperature gradient as areas of niobium approach transition temperature, and hence on details of the cooldown process. Some fraction of flux surrounding the cavity is typically trapped during transition to superconductivity. Rapidly cooling a cell or cavity, so as to produce a spatial temperature gradient in the niobium, can create an advancing boundary between normal and superconducting niobium that expels most of the ambient flux from the superconducting material and minimizes flux trapping. Though fast cooldown itself generates thermoelectric currents and hence transient B fields, the net result is an overall improvement in Q; this has been demonstrated in tests of single cavities and LCLS-II cryomodules.

To reduce reliance on flux expulsion, LCLS-II cryomodules have design features intended to shield the cavities from ambient B fields [13], including a double layer of high-permeability shielding, elimination of ferromagnetic materials near the cavities and reduction of

ISBN: 978-3-95450-184-7 doi:10.18429/JACoW-IPAC2018-MOYGB2

ambient field by demagnetization of the vacuum vessels. These measures have resulted in static fields at and below the goal of 5 mG at the cavities. Active cancellation of ambient fields in the SLAC tunnel is being considered.

Flux Expulsion and Metallurgical Properties

Two vendors supplied niobium and two vendors provided production cavities for LCLS-II. The suppliers were different from those used for the prototypes; however, all four provided satisfactory products to the European XFEL. Nitrogen doping was performed by the cavity vendors to LCLS-II specifications. The cavities for the first production cryomodules exhibited lower-than-target Q, averaging 2.3 x 10^{10}. These results were very good in comparison to state of the art but fell short of LCLS-II targets. The LCLS-II collaboration found itself engaged in cavity R&D again while the cavity fabricators continued production of cavities. It became clear that the variation in flux expulsion had some correlation to grain size in the niobium sheets used to fabricate cavities. Working with cavity vendors, the collaboration made on-the-run modifications to the recipe for the final bake/dope sequence, raising the bake temperature by steps to as high as 975 C (depending on the grain size and hardness of the niobium sheets) prior to nitrogen doping, for which the temperature was always reduced to 800 C. This treatment did increase grain size to some extent and it did dramatically improve flux expulsion for all batches of niobium. As a result, LCLS-II will be built with cavities having a range of Q values.

In order to ensure that LCLS-II will be capable of 4 GeV operation with 4 kW cooling at 2 K, cavities that received sub-optimal bake during early production will be removed from their helium vessels and reprocessed to higher temperatures. FNAL also determined that a faster fast cooldown from 15 K to below 9 K, increasing from 30 gm/sec to as much as 80 gm/sec, could improve flux expulsion for cryomodules built with cavities completed before revising the processing recipe for optimum bake temperature. The project will place cryomodules that would benefit from faster fast cooldown in the LCLS-II linac, where this can be conveniently accomplished without affecting neighboring cryomodules. The LCLS-II project will continue its emphasis on the importance of operating at 4 GeV with a single 4 kW cryoplant.

Undulators

The original LCLS undulator must be replaced by two new undulator X-ray sources. Parameters of the undulators for the hard and soft X-ray undulators are listed in Table 1. Hard and soft X-ray undulator lines have provisions for self-seeding modules. Implementation of soft X-ray self-seeding is still under development at the LCLS facility, and as yet is not sufficiently mature for inclusion in the LCLS-II project.

The beam path for the soft X-ray source includes 21 undulators (Fig. 6) of conventional design. Quadrupoles, phase shifters and beam position monitors are mounted together on a pedestal between undulators. The soft X-ray undulator was designed and acquired by LBNL.

Much of the original fixed-gap LCLS undulator system will be replaced by a new hard X-ray source including 32 horizontal gap/vertical polarization undulators, or HGVPRs (Fig. 7). The existing hard X-ray self-seeding module will be modified to work at high repetition rate.

As the name HGVPU suggests, this source will produce vertically polarized radiation. This undulator design is compact and permits re-use of hardware and controls software developed for LCLS. Since the HGVPU and its associated quadrupole/steering corrector and beam position monitor are all rigidly attached to a single girder mounted on cam movers, the new undulator system can be aligned using the methods and algorithms developed for the fixed-gap LCLS undulators.

Table 1: LCLS-II Undulator Parameters

Parameter	SXU Values	HXU Values	Unit
Undulator period length (λ_u)	39	26	mm
Segment length	3.4	3.4	m
Number of effective periods per segment (N_p)	87	130	
Number of poles per segment	174	260	
Undulator type	Planar	Planar	
Undulator magnet type	PM Hybrid	PM Hybrid	
Gap type	Variable	Variable	
Magnet material	$Nd_2Fe_{14}B$	$Nd_2Fe_{14}B$	
Linear polarization direction of the xray radiation	horizontal	vertical	
Magnetic Field Symmetry	antisymmetric	antisymmetric	
Minimum operational magnetic gap	7.2	7.2	mm
Maximum operational magnetic gap	22	20	mm
On-axis vertical effective field at min. oper. Gap	>1.49	>1.01	T
K_{eff} at minimum operational gap	>5.43	>2.44	
Minimum full open gap	100	100	mm
Minimum operational K values	1.24	0.44	

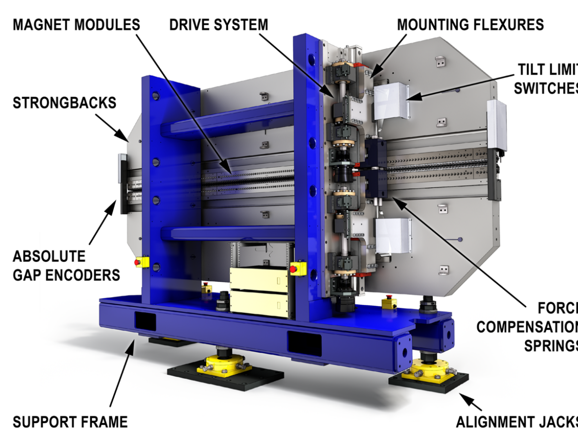

Figure 6: A soft X-ray undulator module.

The magnet poles retain alignment and hence field quality in the presence of the strong, variable attractive force of the magnet poles with the assistance of distributed variable-rate springs that precisely cancel the gap-dependent forces. Vertically polarized radiation can be deflected in the horizontal plane through large angles by

ISBN: 978-3-95450-184-7 doi:10.18429/JACoW-IPAC2018-MOYGB2

crystal optics with significantly better transmission for photon energies below about 7 keV. This is particularly important for the X-ray photon correlation spectroscopy (XPCS) experiment station at LCLS, which measures intensity of X-rays scattered horizontally at angles as high as 55 degrees from crystalline and non-crystalline samples. This experiment can realize as much as a five-fold increase in signal for X-rays scattered at large angles [14].

The HGVPU concept, invented and prototyped at ANL [15] proved that compensation of magnetic forces with nonlinear springs can be employed to produce a compact undulator that satisfies the stringent phase shake specification of an FEL; however, extra care must be taken to eliminate or control other forces on these small cross-section magnet strongbacks. In particular, a very small difference in this undulator will receive electrons from either the new superconducting linac or the 17 GeV 120 Hz LCLS linac. Using the copper linac, the hard X-ray source can provide X-ray energies up to 25 keV.

Thermal expansion coefficients of the aluminum alloys used for the magnet module and strongback resulted in a bimetallic strip effect that affected field quality. This has been remedied for LCLS-II by placing flexures between the module and strongback to reversibly accommodate a small amount of differential expansion.

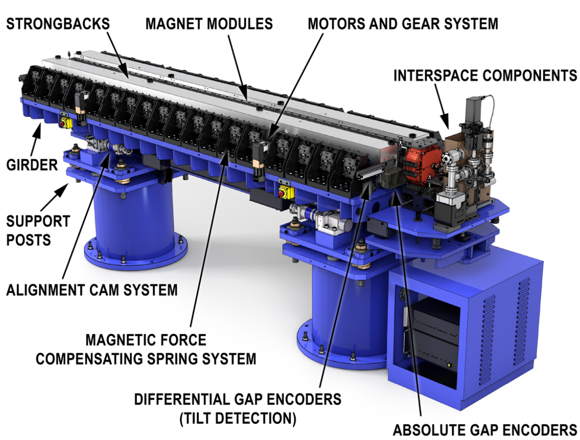

Figure 7: The hard X-ray horizontal gap vertical polarization undulator (HGVPU).

Noteworthy Progress in Other Areas

This paper has focused on innovations such as nitrogen doping and vertical polarization undulators (Fig. 8), which presented the project with opportunities paired with problems and surprises that have been identified and solved in the past year. Other areas of project activity are equally noteworthy, such as the ground-breaking work done on development of low-level RF and resonance control capable of keeping these high-Q cavities on resonance in the presence of microphonics [16].

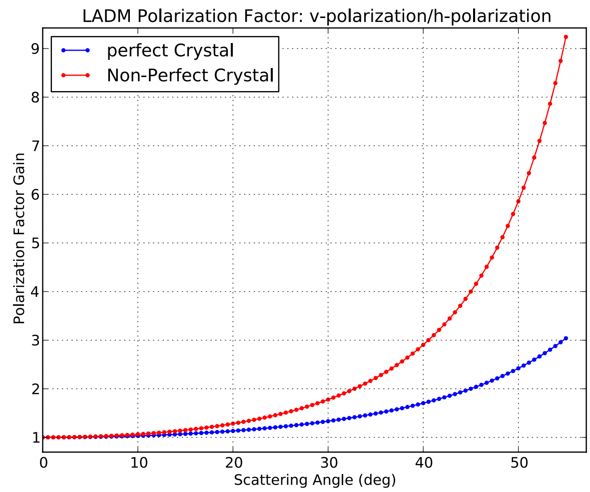

Figure 8: Comparison of signal enhancement versus scattering angle (in the horizontal plane) for perfect (blue line) versus imperfect (red line) samples provided by vertically polarized X-rays in the LCLS X-ray photon correlation spectroscopy (XPCS) station.

ACKNOWLEDGMENTS

I am grateful to the IPAC Conference organizing committee and program committee for inviting me to speak, D. Fritz and D. Arbelaez for their graphics, V. Ravindranath and D. Gonnella for technical review, and R. Kong and G. Chui for editing. I am also grateful to the LCLS-II collaboration for their dedication and creativity, and for the privilege of representing them and a small portion of their work at this conference. I thank SLAC and DOE for their support of the project and of my efforts. Finally I gratefully acknowledge the European XFEL and DESY for invaluable help and advice in numerous areas related to the superconducting linac.

REFERENCES

[1] C. Bostedt *et al.*. (2016), “Linac Coherent Light Source: The first five years,” *Reviews of Modern Physics*, 88. 10.1103/RevModPhys.88.015007

[2] Report of the BESAC Subcommittee on Future X-Ray Light Sources, July 25, 2013 https://science.energy.gov/~/media/bes/besac/pdf/Reports/Future_Light_Sources_report_BESAC_approved_72513.pdf

[3] LCLS-II Conceptual Design Report, SLAC-R-1092, http://slac.stanford.edu/pubs/slacreports/reports09/slac-r-1092.pdf

[4] P. Emma *et al.*, “Linear accelerator design for the LCLS-II FEL facility”, *Proceedings of FEL2014*, Basel, Switzerland, pp. 743-747, THP025.

[5] M. Leitner *et al.*, “Hard X-Ray and Soft X-Ray undulator segments for the Linear Coherent Light Source upgrade (LCLS-II) project”, *Proceedings of IPAC2017*, Copenhagen, Denmark, pp. 1605-1607, TUPAB123.

[6] J. A. Doyle *et al.*, “Development of the manufacturing and QA Processes for the LCLS-II injector source VHF electron gun”, *Proceedings of IPAC2017*, Copenhagen, Denmark, pp. 2815-2817, WEPAB099.

ISBN: 978-3-95450-184-7 doi:10.18429/JACoW-IPAC2018-MOYGB2

[7] F. Zhou *et al.*, "LCLS-II injector physics design and beam tuning", *Proceedings of IPAC 2017*, Copenhagen, Denmark, pp. 1655-1658, TUPAB138.

[8] T. Peterson *et al.*, "LCLS-II 1.3 GHz cryomodule design – modified TESLA-Style cryomodule for CW operation", *Proceedings of SRF2015*, Whistler, BC, Canada, pp. 1417-1421, THPB119.

[9] N. Solyak *et al.*, "Performance of the First LCLS-II cryomodules: issues and solutions", *Proceedings of IPAC 2018*, Vancouver, Canada, MOXGBD3, these proceedings.

[10] N. Huque, E. F. Daly, and Y. Pischalnikov, "Results of accelerated life testing of LCLS-II cavity tuner motor", *Proceedings of SRF2017*, Lanzhou, China, pp. 323-327, MOPB110.

[11] V. Ravindranath *et al.*, "Process simulations for the LCLS-II cryogenic systems", IOP Conference Series: Materials Science and Engineering, Volume 278.

[12] D. Gonnella *et al.*, "RF performance of nitrogen-doped production SRF cavities for LCLS-II", *Proceedings of IPAC2017*, Copenhagen, Denmark, MOPVA128.

[13] S. K. Chandrasekaran, A. Grassellino, C. Grimm, and G. Wu, "Magnetic field management in LCLS-II 1.3 GHz cryomodules", *Proceedings of LINAC2016*, East Lansing, Michigan USA, pp. 527-530, TUPLR027.

[14] David Fritz, private communication, October 2015

[15] N.Strelnikov, I.Vasserman, J.Xu, and E.Gluskin, "Performance of the 3.4-meter long vertical polarizing undulator prototype for LCLS-II", *Proceedings of NAPAC2016*, pp. 946-949, WEPOB23.

[16] L.Doolittle *et al.*, "High precision RF control for SRF Cavities in LCLS-II", *Proceedings of SRF 2017*, Lanzhou, China, pp. 944-950, FRXBA02.